



Supplement of

Zonally asymmetric influences of the quasi-biennial oscillation on stratospheric ozone

Wuke Wang et al.

Correspondence to: Ming Shangguan (shanggm@cug.edu.cn)

The copyright of individual parts of the supplement might differ from the article licence.

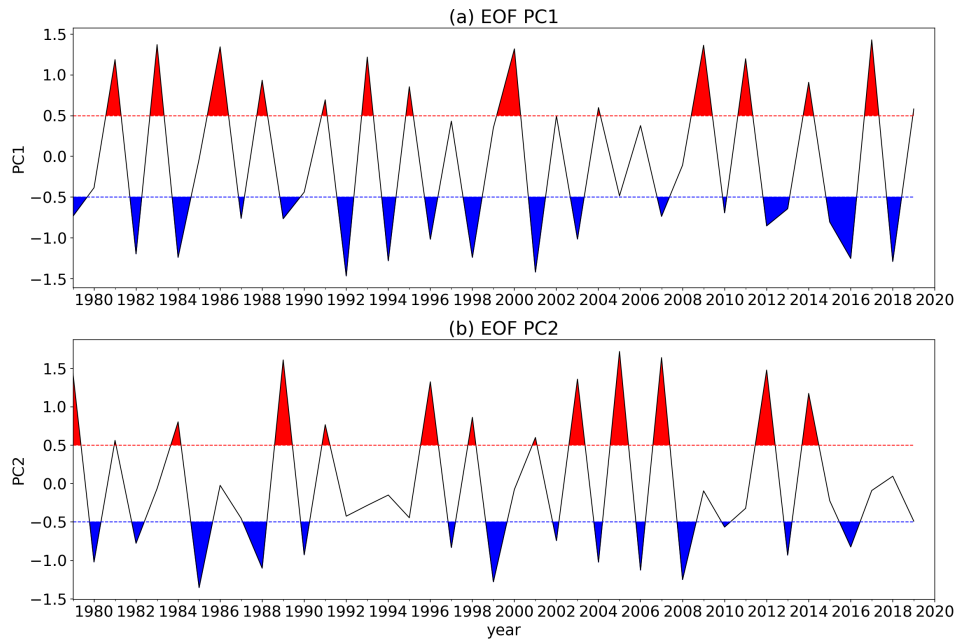


Figure S1: Time series of the QBO index in boreal winter (DJF) from 1979 to 2020, which are the first two principal components (PCs) of the EOF analysis applied to the FUB QBO data from 70 to 10 hPa. **(a)** PC1, indicating the QBO phase in the middle stratosphere at ~ 20 hPa. **(b)** PC2, indicating the QBO phase in the lower stratosphere at 50 hPa. Red/blue colours are shaded where the QBO indexes are greater/less than half of its standard deviation, indicating the QBOW/QBOE phases.

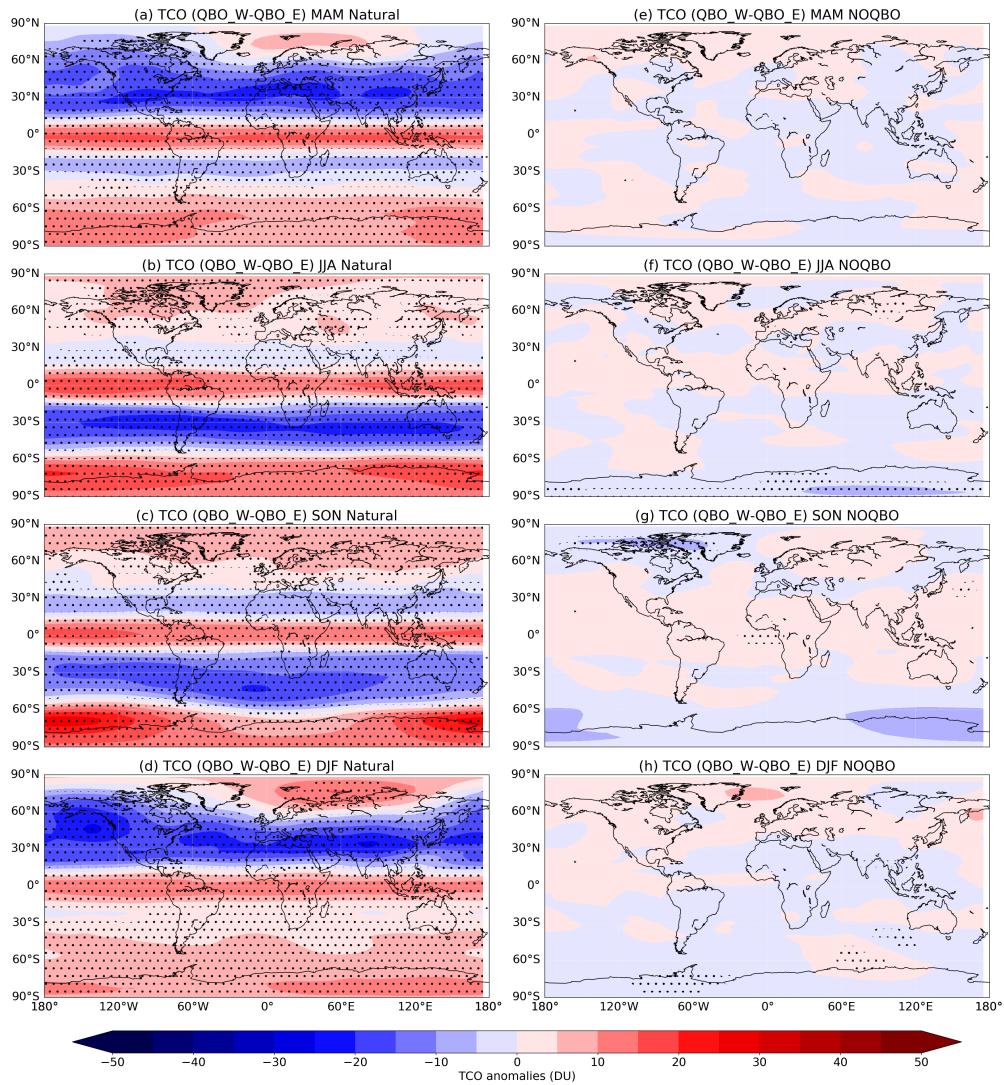


Figure S2: Influences of QBO (QBOW-QBOE) on global total column ozone (TCO) in different seasons based on the Natural **Left** and NOQBO (**Right**) simulations for the period 1955-2099. **(a, e)** MAM. **(b, f)** JJA. **(c, g)** SON. **(d, h)** DJF. Stippled areas indicate results that are statistically significant over the 95% level, using the two-tailed Student's t-test.

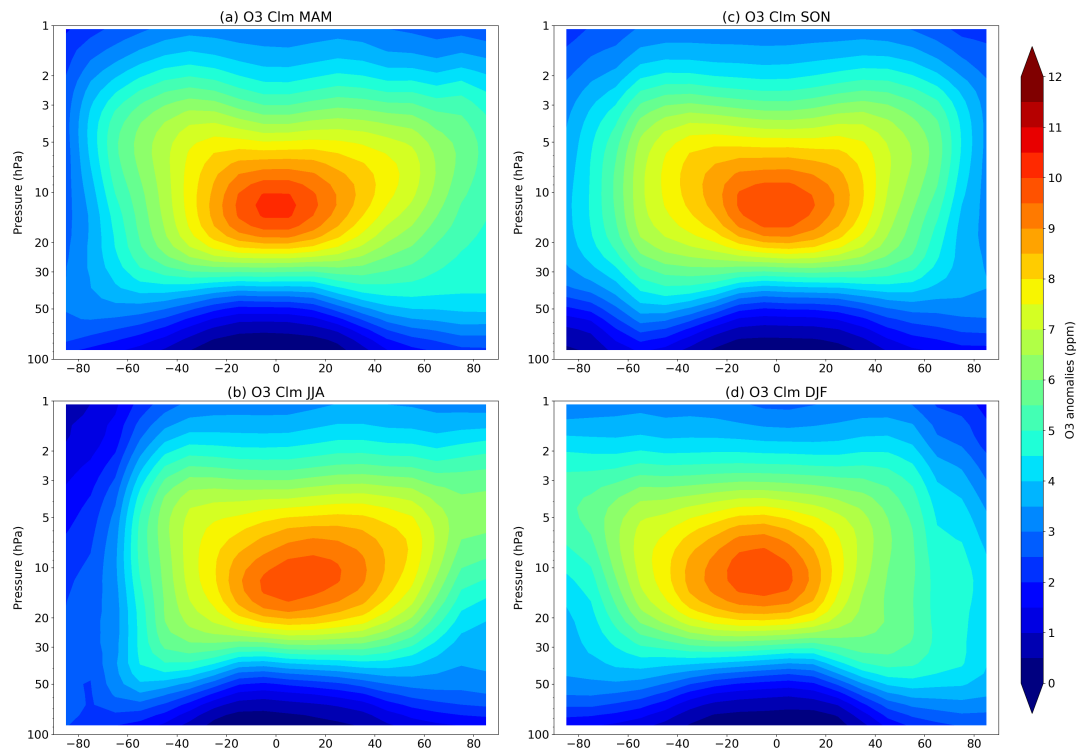


Figure S3: Latitude-height cross-section of the climatological ozone mixing ratios from the merged satellite data from C3S averaged for the period 1985-2020. (a) MAM. (b) JJA. (c) SON. (d) DJF.

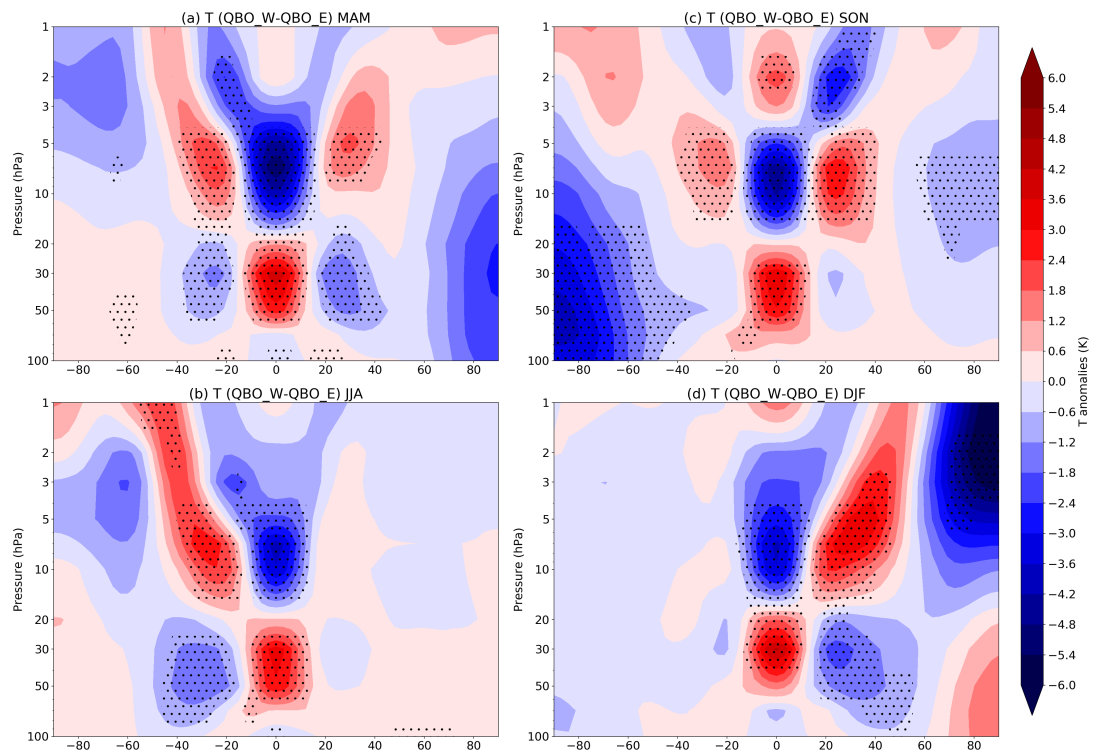


Figure S4: Latitude-height cross-section of the influences of QBO (QBO_W-QBO_E) on temperature from the ERA5 data for the period 1979-2020. **(a)** MAM. **(b)** JJA. **(c)** SON. **(d)** DJF. Stippled areas indicate results that are statistically significant over the 95% level, using the two-tailed Student's t-test.

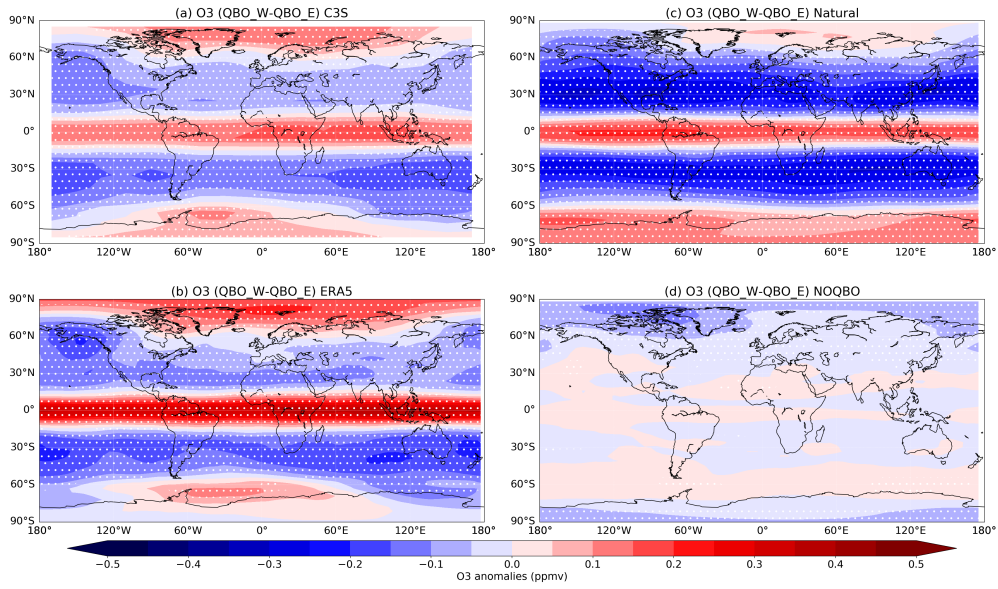


Figure S5: Influences of QBO (QBOW-QBOE) on global lower stratospheric ozone (50 hPa) based on monthly anomalies from different data sets for the period 2002-2020. **(a)** Merged satellite data from C3S. **(b)** ERA5 data. **(c)** CISM-WACCM Natural run. **(d)** CISM-WACCM NOQBO run. Stippled areas indicate results that are statistically significant over the 95% level, using the two-tailed Student's t-test.

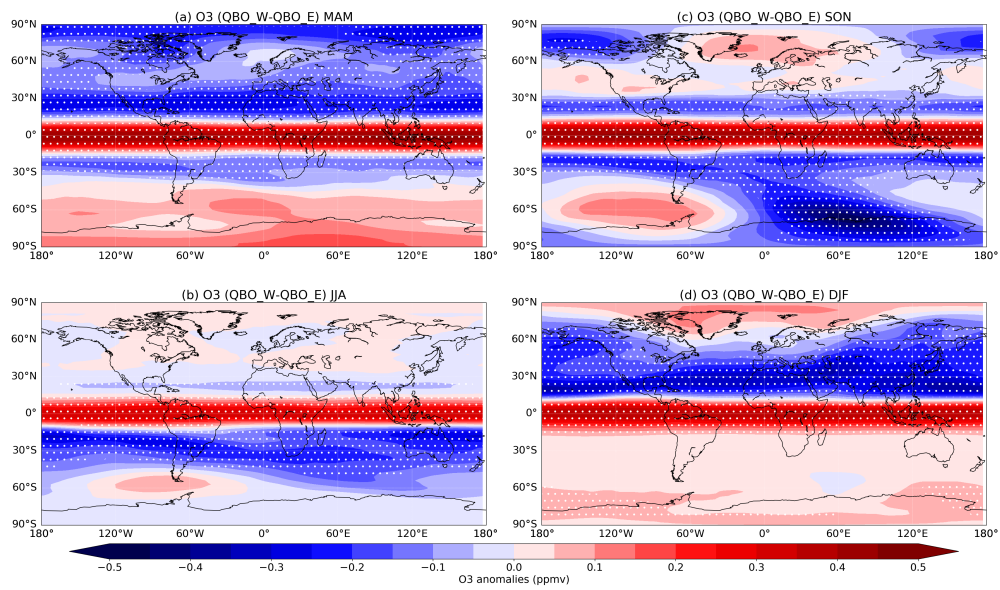


Figure S6: Influences of QBO (QBOW-QBOE) on global stratospheric ozone (10 hPa) based on ERA5 data for the period 1979-2020. **(a)** MAM. **(b)** JJA. **(c)** SON. **(d)** DJF. Stippled areas indicate results that are statistically significant over the 95% level, using the two-tailed Student's t-test.

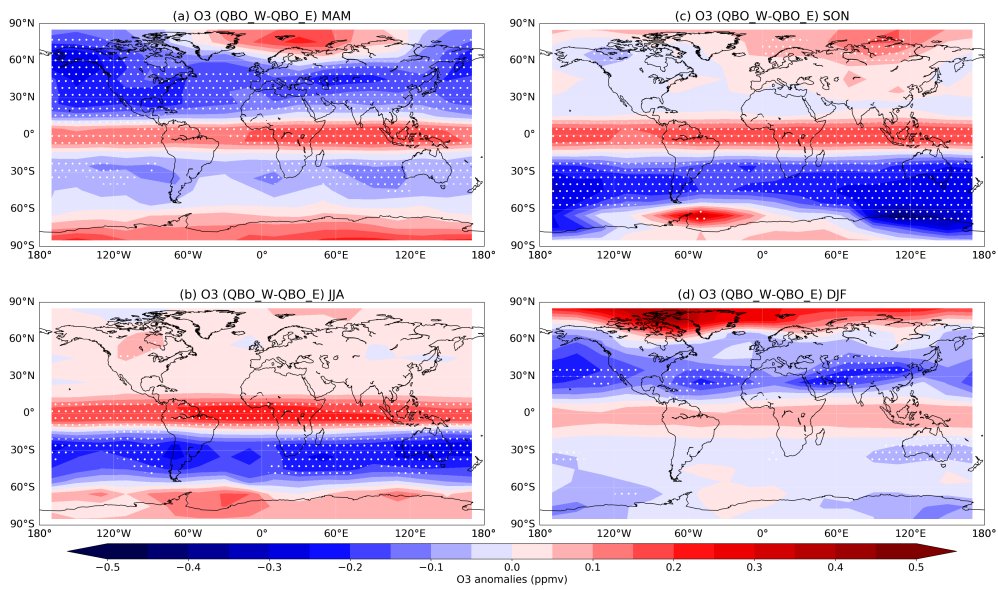


Figure S7: Influences of QBO (QBOW-QBOE) on global lower stratospheric ozone (at 50 hPa) based on merged satellite data from C3S for the period 2002-2020. (a) MAM. (b) JJA. (c) SON. (d) DJF. Stippled areas indicate results that are statistically significant over the 90% level, using the two-tailed Student's t-test.

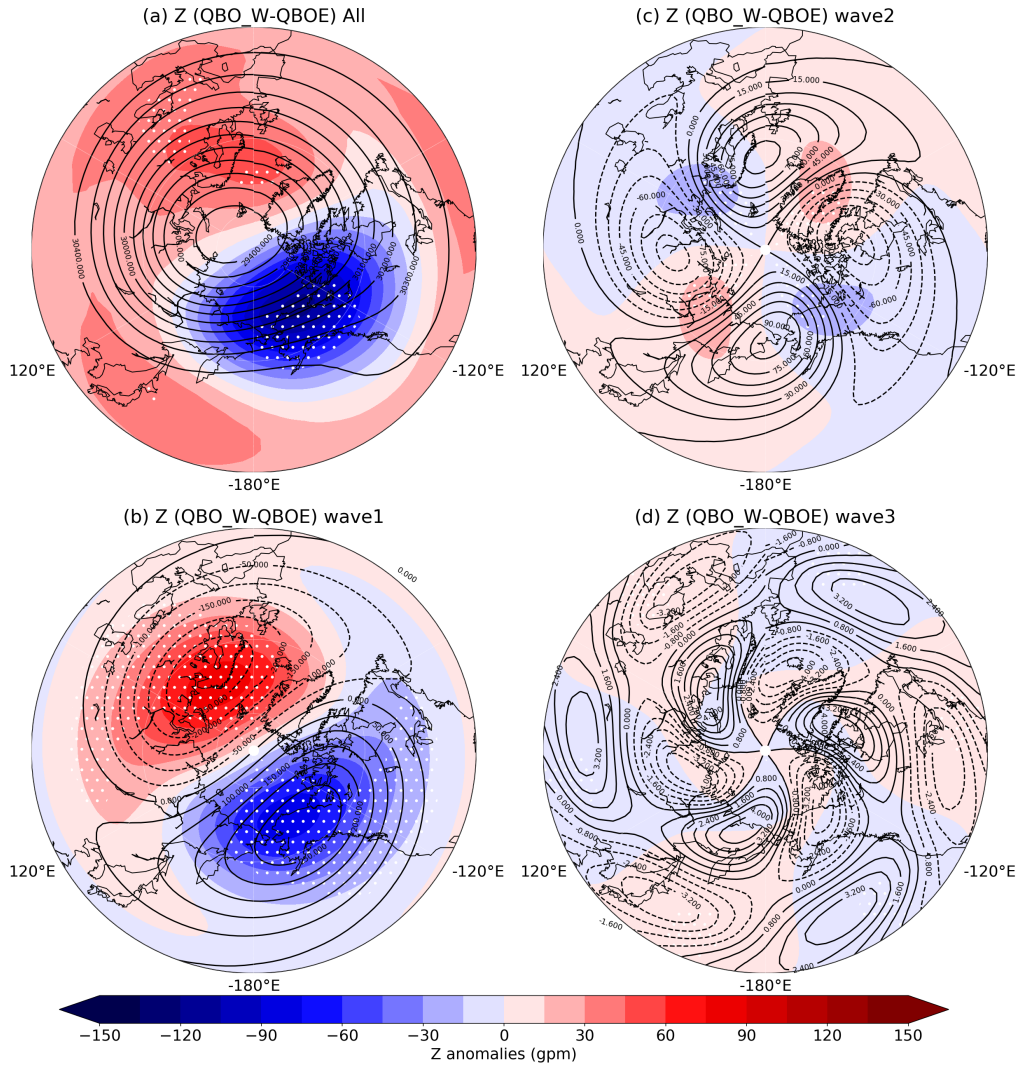


Figure S8: **(a)** Influences of QBO (QBO W-QBOE) on geopotential height (Z at 10 hPa) in the northern hemisphere autumn (SON) based on ERA5 data for the period 1979-2020. **(b-d)** The corresponding changes of geopotential height associated with QBO in wave numbers 1-3. The climatological values of geopotential height during QBOE in winter as well as the climatological patterns of wave numbers 1-3 are also shown (contour lines, with contour intervals of 100, 50, 15 and 0.8 gpm in **(a)**, **(b)**, **(c)**, and **(d)**, respectively). Stippled areas indicate results that are statistically significant over the 95% level, using the two-tailed Student's t -test.

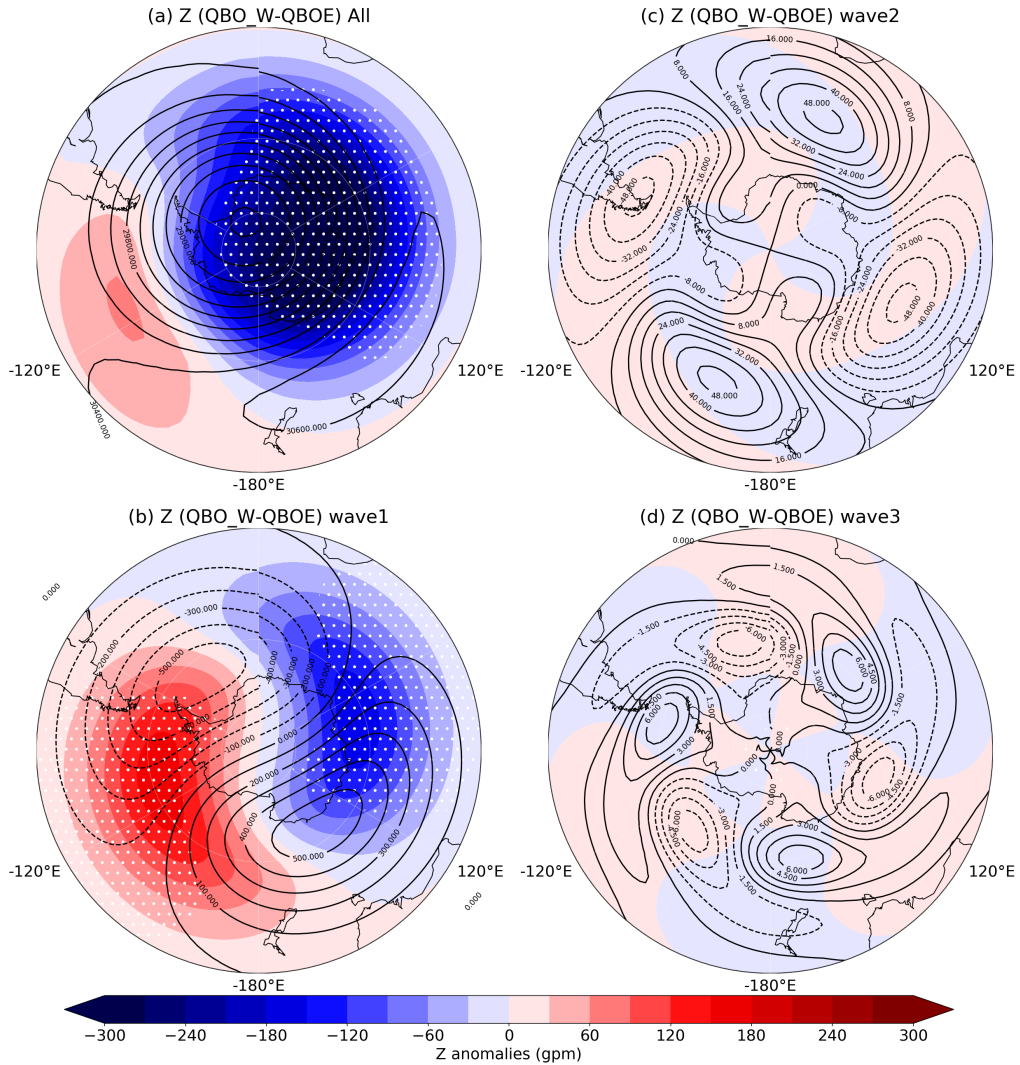


Figure S9: **(a)** Influences of QBO (QBO W-QBOE) on geopotential height (Z at 10 hPa) in the southern hemisphere spring (SON) based on ERA5 data for the period 1979-2020. **(b-d)** The corresponding changes of geopotential height associated with QBO in wave numbers 1-3. The climatological values of geopotential height during QBOE in winter as well as the climatological patterns of wave numbers 1-3 are also shown (contour lines, with contour intervals of 200, 100, 8 and 1.5 gpm in **(a)**, **(b)**, **(c)**, and **(d)**, respectively). Stippled areas indicate results that are statistically significant over the 95% level, using the two-tailed Student's t -test.

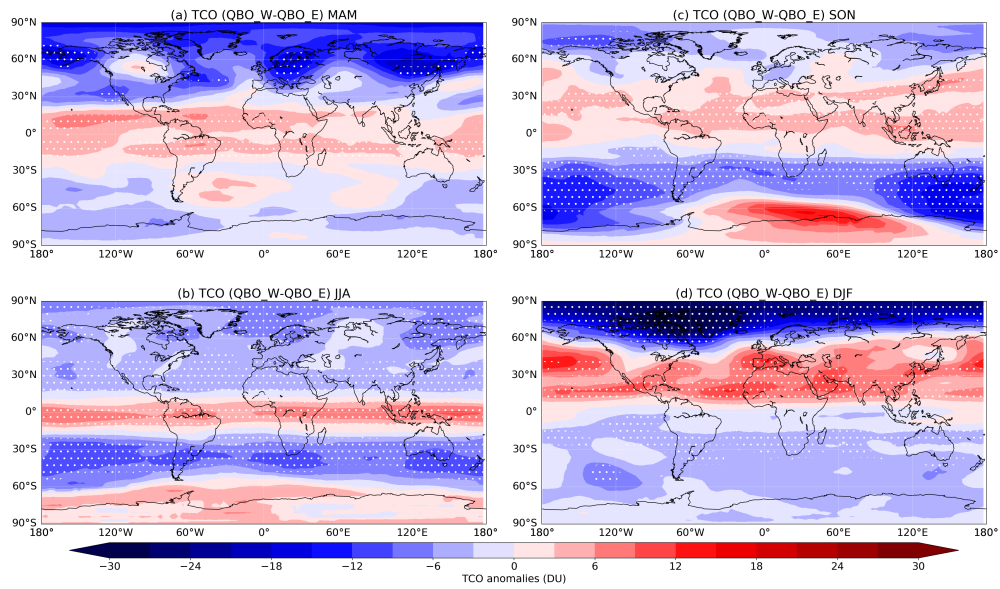


Figure S10: Influences of QBO (QBOW-QBOE, using a QBO index at 50 hPa) on global total column ozone (TCO) in different seasons based on MSR2 data 1979-2020. (a) MAM. (b) JJA. (c) SON. (d) DJF. Stippled areas indicate results that are statistically significant over the 95% level, using the two-tailed Student's t-test.